



# NIH Public Access

## Author Manuscript

*Langmuir*. Author manuscript; available in PMC 2013 November 27.

Published in final edited form as:

*Langmuir*. 2012 November 27; 28(47): 16338–16346. doi:10.1021/la303237u.

## Flagellar display of bone protein-derived peptides for studying peptide-mediated biomineralization

**Dong Li, Salete M. C. Newton, Philip E. Klebba, and Chuanbin Mao\***

Department of Chemistry & Biochemistry, Stephenson Life Sciences Research Center, University of Oklahoma, Norman, Oklahoma 73019

### Abstract

Bacterial flagellum is self-assembled primarily from thousands of a protein subunit called flagellin (*FliC*). A foreign peptide can be fully displayed on the surface of the flagellum through inserting it into every constituent protein subunit. To shed light into the role of bone proteins during nucleation of hydroxyapatite (HAP), representative domains from type I collagen, including a part of N-, C-terminal, N-, C-zone around hole zone and a 8 repetitive Gly-Pro-Pro (GPP8) sequence similar to central sequence of type I collagen, were separately displayed on the surface of the flagella. Moreover, eight negatively charged, contiguous glutamic acid residues (E8) and two other characteristic sequences, derived from a representative non-collagenous protein called bone sialoprotein (BSP), were also displayed on flagella. After being incubated in a HAP supersaturated precursor solution, flagella displaying E8 or GPP8 sequences were found to be coated with a layer of HAP nanocrystals. Very weak or no nucleation are observed on flagella displaying other peptides being tested. We also found that calcium ions can induce the assembly of the negatively charged E8 flagella into bundles mimicking collagen fibers, followed by the formation of HAP nanocrystals with the crystallographic c-axis preferentially aligned with long axes of flagella which is similar to that along the collagen fibrils in bone. This work demonstrates that due to the ease of peptide display on flagella and self-assembly of flagella, flagella can serve as a platform for studying biomineralization and as a building block to generate bone-like biomaterials.

### Keywords

bacterial flagella; biomimetic nucleation; hydroxyapatite; assembly; nanobiomaterials; nanofiber

A biocompatible and biodegradable scaffold is desired for bone repair and regeneration. New bone can be built on such scaffold and finally defective bone tissue can be replaced.<sup>1</sup> However, constructing a nanocomposite mimicking both the composition and the organization of bone is still challenging. The extracellular matrix (ECM) in bone is mainly composed of inorganic mineral-hydroxyapatite (HAP,  $\text{Ca}_{10}(\text{PO}_4)_6(\text{OH})_2$ ) and organic matrix primarily made of type I collagen.<sup>2</sup> From a materials science point of view, bone tissue is an inorganic-organic hybrid nanocomposite material containing multiple levels of hierarchical structures. At the lowest level, the HAP nanocrystallites (20–80 nm long, 2–5 nm thick) are assembled along the fibrous collagen molecules.<sup>3–5</sup> With the development of tissue engineering, especially combined with nanotechnology, designing artificial biomaterials at the nanoscale to interact with and replace ECM becomes feasible.<sup>3, 6</sup> In contrast with the

\*Corresponding Author. Address correspondence to cbmao@ou.edu.

#### ASSOCIATED CONTENT

Supporting Information: Peptide sequences and positions displayed on flagella, morphology of flagella, nucleation of flagella displaying N- and C-zone sequences, bundle formation induced by  $\text{CaCl}_2$ , FTIR analysis and TEM images of nucleated super-flagella. This material is available free of charge via the Internet at <http://pubs.acs.org>.

conventional methods, these novel materials can mimic the complex and delicate structure of bone, which are developed and synthesized at the nanoscale level via a “bottom up” approach. Hybrid molecular biomimetics are emerging as a promising methodology.<sup>7</sup> Recently, we demonstrated the oriented nucleation of HAP nanocrystals on natural occurring nanomaterials.<sup>8–10</sup> In this study, using peptide display technique, the bioengineered flagella were used as a platform to test the HAP nucleation capability of the peptides derived from bone proteins. At the same time, flagella were also used as novel “smart” basic building blocks to build composite biomaterials structurally mimicking the nanoscale level of bone structures.

The bacterial flagellum is a long nanotube-like filament composed of several thousand copies of the eubacterial flagellin (*FliC*) major proteins as well as some other minor proteins such as a pentamer of the *FliD* protein capping the tip of the flagellum (Scheme 1A). Bacterial *FliC* monomers naturally self-assemble into a linear tube with a repeat of about 11 monomers per two turns via noncovalent interactions between the  $\alpha$ -helical and coiled-coil motifs of neighboring flagellin.<sup>11</sup> Each flagellum is about 10–20  $\mu\text{m}$  in length with an outer diameter of 12–25 nm and an inner diameter of 2–3 nm. The length of the flagellum is tunable, depending on the number of monomers. The N- and C-terminal region of *FliC* located in the inner tube are highly conserved, whereas the central region of *FliC* is surface-exposed and contains highly variable sequences. A foreign peptide can be inserted into the variable region of flagellin through genetic engineering, leading to the display of this foreign peptide on the surface of flagella. As long as 302 amino acid residues were successfully displayed on flagella.<sup>12</sup> This is a major advantage over phage display because only shorter peptides (e.g., shorter than 20-mer) can be displayed on the side wall of phage with high density.<sup>8</sup> Traditionally, the recombinant bacterial flagella were used as live vaccines to evoke humoral and cellular immune responses.<sup>13</sup> Recently, the bioengineered flagella directed synthesis of inorganic and organic nanotubes has been reported<sup>14–19</sup>. However, there has been no research on the use of flagella to understand which bone protein-derived peptides can nucleate HAP and the cation-induced self-assembly of flagella.

In bone tissue, type I collagen molecules are parallel to each other forming thicker fibrils in a hexagonal array. The type I collagen molecules align with each other and pack precisely into the so-called quarter-staggered mode exhibiting a characteristic D-banding, which exhibits the alternating hole or gap (47 nm in length) and overlap (20 nm in length) zones.<sup>20</sup> Biominerization occurring on the collagen fibrils involves the nucleation, growth and assembly of HAP nanocrystals in the appropriate microenvironment. To date, however, the direct evidence and precise chemical mechanisms of HAP nanocrystal nucleation are still not clear. Most of the previous reports suggest that HAP nanocrystals are initially nucleated at the hole zone of the collagen fibrils,<sup>20, 21</sup> specifically at the defined region -e and -d bands, which contain charged amino acid side chains.<sup>22</sup> However, Maitland and Arsenault<sup>23</sup> found nucleation of HAP crystals occurred in both the hole and overlap zones during early stage of mineralization in an asymmetric pattern. *In vitro*, type I collagen can also nucleate the HAP nanocrystals by itself,<sup>22</sup> but it is still a mystery to be clarified, which domain of type I collagen directs the initial nucleation and determines the nucleation sites of HAP within hole or overlap zones. The potential sites of HAP nucleation may occur on the charged amino acid residues of the type I collagen including glutamic and aspartic acid, lysine, arginine, hydroxylysine and histidine.<sup>24</sup> Accordingly, in this work peptides derived from the complete N-, C-terminals and partial N-, C-zones enriched of polar amino acid residues are displayed on flagella to clarify the nucleation roles of collagen (Scheme 2). Because the biominerization is also possibly initiated at both of the hole and overlap zones, an 8 repetitive Gly-Pro-Pro (GPP8) sequence similar to type I collagen main composition Gly-X-Y (where X is often proline and Y is often hydroxyproline) is designed

to be displayed on flagella (Table 1) and the relative positions of these sequences are depicted in Figure S1.

It is well established that type I collagen itself is not the only contributor for HAP nucleation in actual bone biominerization. Many non-collagenous proteins, which control the nucleation and the growth of the mineral phase, are considered to be important factors in the biominerization process.<sup>25–27</sup> Osteopontin (OPN), BSP and osteocalcin (OCN) are the prominent non-collagenous proteins that are thought to regulate of HAP nucleation due to the presence of the acidic amino acids.<sup>28, 29</sup> As a very important nucleator, BSP can bind to collagen, forming a complex as a nucleator to induce the nucleation of HAP crystals.<sup>30</sup> Moreover, x-ray crystal structure of OCN indicates that it coordinates with 5 calcium ions in a spatial orientation corresponding to calcium ion positions in the HAP crystal lattice.<sup>29</sup> He *et al*<sup>31</sup> reported dentin matrix protein 1 (DMP1), which is also an acidic non-collagenous protein, could nucleate HAP *in vitro*. *In vivo*, non-collagenous proteins are morphologically, structurally, and functionally integrated with the collagen fibrils, which facilitate primary crystal formation and subsequent crystal growth. A possible mechanism is that anionic groups on non-collagenous proteins produce a local supersaturation of inorganic cations, primarily Ca<sup>2+</sup> among other ions, especially in intermolecular β-sheet acidic domains.<sup>31–35</sup> Therefore, we also displayed a peptide constituted by 8 glutamic acid residues (E8) and two other sequences enriched in acidic amino acids (named BSP1 and BSP2) from BSP on flagella (Table 1).

Studying the nucleation of flagella displaying different bone protein-derived peptides in a supersaturated HAP solution may provide us with more information on which domains of bone related proteins serve as nucleators and promote the nucleation process. The biomimetic process utilized here, in which HAP nanocrystals are nucleated on the surface of the engineered flagella, can not only be used to test the nucleation by different peptides displayed on flagella, but also lead to the production of materials that are structurally similar to natural bone structures at the nanoscale level. This research may result in a new approach to designing artificial bone ECM that can find potential application in bone repair or regeneration.

## EXPERIMENTAL SECTION

### Preparation of DNA fragments

The single-stranded oligonucleotides that encode target peptides including restriction sites of *Xho*I and *Bgl*II were synthesized (Invitrogen). The primers were then annealed (100 mM) to form complementary double-stranded DNA with a restriction site of *Xho*I at the 5'-end as well as *Bgl*II site at the 3'-end. The full DNA and protein sequences from type I collagen and BSP displayed on flagella are listed in Table 1.

### Peptide display on flagella surface

The vector pLS411 contains the gene for a flagellin protein in which most of the central hypervariable region has been deleted and replaced with a 45 bp oligonucleotide encoding a foreign peptide (Cholera toxin peptide 3, CPT3). This epitope is inserted by restriction sites *Xho*I and *Bgl*II<sup>13</sup>. After purification of *Xho*I and *Bgl*II linearized vector pLS411, the double-stranded oligonucleotides were ligated by T4 ligase (Invitrogen). Finally, the recombinant plasmids were transformed into flagellin deficient *Salmonella* strain SL5928 by electroporation. SL5928 is an aroA live-vaccine strain of *Salmonella* Dublin. Because its only flagellin gene, *FliC*(g, p), has been replaced via transduction by *FliC*(i)::Tn10, an allele inactivated by transposon insertion, the functional flagella cannot be expressed.

## Purification of bacterial flagella

SL5928 with recombinant plasmid was inoculated into semisolid medium (1% tryptone; 1.5% NaCl; 0.35% agar) and incubated at 37 °C until it reached the edge of the plate. The cells from the advancing edge of growth were inoculated into 1 L of LB containing L-ampicillin (100 µg/mL) and incubated at 37 °C with shaking (250 rpm). When the OD of the cell culture reached about 0.6–0.8, the cultured bacteria were harvested by centrifugation at 6000 g for 15 min, washed three times with phosphate-buffered saline (PBS, pH 7.2). The flagella were detached from the bacterial cells by vigorous vortex at the highest speed for 3 times (30 sec/each time). The supernatant containing the sheared flagella was separated by centrifugation at 12,000 × g for 15 min.

## Flagella examination

Flagella were examined with silver staining under bright field microscopy. The purified flagella were also negatively stained with 1% (wt/vol) uranyl acetate (UA) and characterized with transmission electron microscopy (TEM, Zeiss 10).

## Western blot analysis

The displayed peptides of GPP8 and E8 on flagella were probed with the polyclonal antibody, rabbit anti-type I collagen or rabbit anti-BSP (1:1000 dilution) respectively (Sigma-Aldrich), followed incubation with alkaline phosphatase-conjugated goat anti-rabbit antibody (Sigma-Aldrich) (1: 2000 diluted in TTBS) for 1 h at room temperature under constant agitation. Finally, the blotting bands were visualized by incubation with chromogenic substrates-NBT/BCIP for 30 min at room temperature in the dark.

## Nucleation of flagella in supersaturated HAP solution

Supersaturated HAP solution (4 mM) was prepared as described<sup>49</sup> from HAP powder (Sigma-Aldrich). The bioengineered flagella (20 µL, 50 µg/mL) were mixed with 500 µL of supersaturated HAP solution and incubated for various periods of time at room temperature. Wild type flagella were used as a control. A drop of mixture was mounted on the carbon TEM grids. After being carefully rinsed with ddH<sub>2</sub>O and air-dried at room temperature, these grids were subjected to TEM (Zeiss 10 and JEOL 2000-FX) measurements.

## Flagella assembly into higher-order structures

The CaCl<sub>2</sub> solution (100 mM) was adjusted to pH=9.5 by NaOH because the flagella are stable at pH=2–10. The solution was then diluted into different concentrations with water. The purified flagella (100 µL, 50 µg/mL) were then added to 500 µL of CaCl<sub>2</sub>. The bundled flagella were collected by centrifugation (10,000 g for 10 min) and washed with water. Finally, the flagella bundles were incubated in supersaturated HAP solution at room temperature.

## RESULTS AND DISCUSSION

*In vivo*, biomineralization of bone is a cell-mediated complex process, which mainly involves deposition of HAP crystalline materials within the ECM in an organized fashion.<sup>26</sup> Although the peptides displayed on flagella surfaces may exhibit different conformations from those in the native bone proteins, we believe the displayed peptides used here can provide more information to aid in the understanding of the nucleation of HAP. Each flagellar filament is a nanofiber assembled from thousands of subunits. Because the *FliC* is organized along the filament during the self-assembly, the peptide inserted into each subunit will be naturally organized and uniformly distributed throughout the surface of flagella (Scheme 1B).<sup>11</sup> By biomimetic nucleation, the displayed peptides which serve as the

nucleator to direct mineral nucleation can be identified. Moreover, the mineralized flagella resemble the lowest level of hierarchical organization of bone in which type I collagen fibrils are mineralized with HAP nanocrystals<sup>4, 22</sup>.

### Peptide display on surface of flagella and characterization

The plasmids were sequenced at each step to confirm the identity of the inserts. The strains with recombinant plasmids were cultured on semi-solid media with a negative control strain SL5928. After incubated at 37 °C for 1 day, all of recombinant strains diffused from the inoculated site, but the negative control SL5928 only formed a colony in the center of the plate due to its lack of motility. Since bacterial cells use flagella as a “propeller” to swim in liquid, the motility assay confirmed that the flagella polymerized from the engineered bacterial flagellin were functional. However, the diffusion speeds of recombinant stains varied from each other as well as from the control. For example, the strain with E8 spread faster than that with GPP8 (Figure S2).

Before and after the bacterial flagella were purified from bacteria, they were examined and verified by light microscopy using silver nitrate staining. Over ten flagella were observed on the surface of a single bacterium at SL5928 with E8 (Figure S3a). After purification, a large amount of flagella with characteristic sinusoidal morphology were observed at a very high degree of purity (Figure S3b). Under TEM, flagella exhibited a more linear structure after staining by uranyl acetate (UA) with 15±0.5 nm in diameter and 2–4 micrometers in length (Figure S3c).

After purification, the recombinant flagella was subjected to SDS-PAGE analysis, which only showed one band with a molecular weight of about 55 kDs on the gel (Figure 1a). This indicated that flagellin was isolated with a very high degree of purity. Bovine serum albumin (BSA) at 66 kDs and SL5930 were used a control. Strain SL5930 is a pBR322 derivative also containing flagellin gene with a 48-bp deletion in hyper variable region.<sup>36</sup> Other recombinant flagella with N-, C-terminal, N-, C-zone inserts also exhibit very similar molecular weight band on the SDS-PAGE gel (data not shown). *FliC* with GPP8 or E8 (1.6 mg/mL, 8 µL/well) against anti-type I collagen and BSP polyclonal antibody showed a very clear blotting band (Figure 1b).

### Biomimetic nucleation of flagella displaying the peptides derived from bone proteins

Flagella are invisible under TEM without mineral nucleation or staining. Thus, being visible under TEM is an easy starting point to verify the formation of minerals on non-stained flagella. After being mineralized in the supersaturated HAP precursor solution for 3, 6 and 9 days, the flagella were examined by TEM. In the control, there was no visible mineralization on wild type flagella until the ninth day. Similar results were observed for the flagella displaying N-, C-terminal peptides. However, a very thin layer of amorphous mineral deposited on the surface of the flagella displaying N-, C-zone inserts and created a low contrast image (Figure S4). The flagella displaying BSP1 and BSP2 also exhibit weak nucleation ability similar to the flagella displaying N-, C-zone inserts (data not shown).

Higher contrast images were observed on flagella with E8 and GPP8 sequences because the flagella were wrapped by a thicker layer of nucleated inorganic minerals after 3 days. From selected area electron diffraction (SAED) analysis, only amorphous minerals were formed at this time (Figure 2a, b). After 6 days, the E8 and GPP8 flagella were shown to be decorated with crystalline minerals which were confirmed by SAED analysis. However, the flagella surfaces were not completely covered by minerals. A lot of gaps can be observed along the flagella (Figure 2c, d). After 9 days, an entire layer of polycrystalline minerals was observed on the flagella displaying E8 and GPP8 sequences with diameters of 46±5 nm and 38±4 nm,

respectively (Figure 2e, f). The increase of diameters of the filamentous structures after mineralization further confirmed the formation of minerals on the surface of flagella. In the SAED patterns, the presence of the (211) and (002) planes indicates that the HAP mineral formed on the surface of flagella is polycrystalline. However, consistent patterns with stronger diffraction rings were observed on E8 flagella than those on GPP8 flagella at each time interval. Interestingly, at higher concentration, E8 flagella (10 µg/mL) show strong tendency to form bundle-like structures after being soaked in supersaturated HAP solution (Figure 3). However, the bundle-like structures were not parallel very well to each other but forming network structures.

The role of collagen in bone mineralization is controversial.<sup>22, 24, 26, 37</sup> The hole zone domain of type I collagen might participate in the process of mineralization.<sup>24</sup> However, the overlap zone was also reported to be involved in the nucleation process of HAP in an asymmetric pattern.<sup>26</sup> Except for these domains, the major portion of type I collagen composed of repeating G-X-Y sequence was proposed to provide the organizational framework and spatial constraint for crystal deposition. The exact role and mechanism of this repeating sequence were not very clear.<sup>26</sup> In this work, different domains from type I collagen were selected and displayed on flagella to elucidate their roles in the nucleation of HAP. Surprisingly, our results showed that among all the type I collagen-derived sequences displayed on flagella, GPP8 exhibited HAP nucleation ability, even still, slightly weaker than E8 (Figure 2). It was reported that proline residues could affect the calcium-binding activity<sup>38</sup> and that CaCl<sub>2</sub> could induce conformational change of poly-prolines.<sup>39</sup> These facts indicated the interaction between proline and Ca<sup>2+</sup>. Most recently, Chung *et al*<sup>40</sup> identified a 12-residue peptide binding to (100) single-crystal HAP that resemble the tri-peptide repeat sequences (Gly-Pro-Hyp) in type I collagen. Moreover, the peptide could mediate HAP nucleation *in vitro* ascribed to the cooperative noncovalent interactions between peptide and HAP. We only surmise a similar mechanism for the nucleation of HAP on flagella displaying GPP8.

No crystals were nucleated on flagella displaying N-, C-terminal domains, so they might not involve the mineralization process even if there are some polar amino acids in the two domains. However, flagella displaying N- or C-zone show weak nucleation capability (Table 1). Specific conformations of protein are very important for HAP nucleation.<sup>24, 31</sup> There are also some polar amino acids in selected sequences of N-, C-zone (Table 1). Moreover, they exhibited tri-peptide (G-X-Y) like structures. Both polar amino acids<sup>22</sup> and collagen like sequences<sup>40</sup> could contribute to the nucleation of inorganic minerals. That is probably why flagella displaying N- or C-zone could nucleate minerals.

During biominerization, many kinds of non-collagenous macromolecular proteins participated in the control of HAP nucleation and growth of the mineral phase. They were present in bone ECM or integrated with the collagen fibers regulating the nucleation of HAP.<sup>26, 41</sup> For example, BSP could bind to collagen to form a complex that served as a nucleator to induce HAP formation.<sup>42</sup> Notably, it had two poly-glutamic acid (poly[E]) regions located in the N-terminal of the molecule. The poly[E] could form an  $\alpha$ -helical structure providing an appropriate spacing of the  $\gamma$ -carboxylate groups for binding Ca<sup>2+</sup> and a sequence of at least eight contiguous glutamic acid residues might be required.<sup>34, 35, 43</sup> Replacement of any single poly[E] domain in BSP with either poly-aspartic acid (poly[D]) or poly-alanine (poly[A]) did not alter its nucleating activity but not both.<sup>44</sup> Here, strong nucleation ability was shown on flagella displaying E8. It was proposed that local ions were highly concentrated at the interface of negatively charged flagella and HAP precursor solution. An initial accumulation of the Ca<sup>2+</sup> on the -COO<sup>-</sup> surfaces resulted in the availability of nuclei through electrostatic interactions followed by PO<sub>4</sub><sup>3-</sup> incorporation,<sup>30, 33-35, 44</sup> finally, leading to *in situ* nucleation of HAP on the flagella.

### Self-assembly of flagella induced by $\text{Ca}^{2+}$ with mineralization

In order to obtain parallel bundles for the purpose of identifying the relative orientation of the mineral crystals with respect to flagella and mimicking the lateral stacking of collagen fibrils to some extent, flagella bundles induced by  $\text{Ca}^{2+}$  were investigated. Divalent metal ions or positively charged polymers could induce protein fibers to aggregate laterally and assemble into net-like paracrystals or side-by-side bundles.<sup>45</sup> Because the E8 flagella exhibited strongest nucleation of polycrystalline minerals (Figure 2) among those tested, they were selected to be assembled into bundles for further analysis. Although  $\text{Ca}^{2+}$  ions tend to electrostatically cross-bridge neighboring anionic E8 flagella into bundles, they can influence the stability of flagella. High concentration of  $\text{CaCl}_2$  (0.5 M) can induce complete depolymerization of flagella.<sup>46</sup> In this study, we found partial depolymerization of the E8 flagella at concentration of  $\text{CaCl}_2$  over 7 mM (Figure S5d). Interestingly, below 7 mM of  $\text{CaCl}_2$ , bundles of flagella were formed in a  $\text{CaCl}_2$  concentration dependent manner. More flagella bundles were observed at higher concentration of  $\text{Ca}^{2+}$  (Figure S5). Finally, 4 mM  $\text{CaCl}_2$  was determined to be optimal and was used for this study (Figure S6). Parallel bundle structures of flagella up to 200 nm in diameter were observed and packed into flat ribbon-like structures losing their characteristic curly morphology.

The interactions between  $\text{Ca}^{2+}$  and flagella displaying E8 were further examined by Fourier transform infrared spectroscopy (FTIR). The peak at  $1657\text{ cm}^{-1}$  predominantly corresponding to the C=O stretch peak in flagella displaying E8 shifted to  $1629\text{ cm}^{-1}$  after the formation of flagella/ $\text{Ca}^{2+}$  complex (Figure S7). The red shift indicates that the C=O bonds in E8 flagella were weakened because of the formation of chelate bonds between  $\text{Ca}^{2+}$  and C=O bonds.<sup>20, 41</sup> This implies that the carbonyl groups on the surfaces of flagella with E8 were ionized by the coordination of  $\text{Ca}^{2+}$ . At the same time, the peak at  $1528\text{ cm}^{-1}$ , corresponding to a combination of the N–H in-plane bend and the C–H stretch, almost disappeared due to the decrease in the total absorption intensity.<sup>20</sup>

The flagella bundles induced by calcium ions were collected by centrifugation. After being carefully washed with pure water, the bundles were immersed in a 4 mM supersaturated HAP solution. After one day, amorphous minerals with tiny inorganic nanoparticles were nucleated and aligned on flagella (Figure 4a). Meanwhile, the flagella bundles became “loose” after soaking in HAP precursor solution. Plate-shaped polycrystalline mineral could be observed throughout the surface of flagella thick bundles after 3 days (Figure 4b). Energy-dispersive X-ray spectroscopy (EDS) revealed a Ca/P ratio of  $1.65 \pm 0.05$ , which is close to the theoretical value of HAP with a formula of  $\text{Ca}_{10}(\text{PO}_4)_6(\text{OH})_2$  ( $\text{Ca}/\text{P} \approx 1.67$ ) (Figure 4d). Some minor Na and Cl were detected which should be precipitated from supersaturated HAP precursor solution. The copper and silicon came from the sample substrates. Narrower mineralized flagella bundles could also be observed on the same TEM sample (Figure 4c). The diffraction arcs corresponding to the (002) and (004) plane demonstrated that the HAP is oriented with its crystallographic *c*-axis preferentially parallel to the long axis of flagella bundles (Figure 4c inset). The preferred orientation of the HAP is consistent with reports on other assembled fibers.<sup>10, 32</sup> The crystallographic orientation of HAP could be controlled by the aligned carboxyl groups.<sup>43</sup> The displayed E8 is also very organized and aligned on the surface of flagella (Scheme I) which could result in the oriented nucleation and growth of HAP. Moreover, the HAP could be nucleated within the channels between neighboring flagella bundles and grow along them. The resultant structure is similar to that of mineralized collagen fibrils in which HAP nanocrystals are also preferentially oriented with their *c*-axis parallel to the long axes of the collagen fibrils.

The ease of inserting a foreign peptide into every subunit *FliC* and the concomitant full display of the peptide on the surface of a 1D nanostructure allow us to use the flagella as a platform to test the nucleation and also as a building block to form higher-order structures.

The flagella can be easily purified in large scale with low cost and it is very important for actual biomedical applications. In addition, the flagella can disassemble into monomers at low pH and reassemble into integrated flagella at pH 7<sup>46</sup> in a fashion similar to the amphiphile fibers.<sup>32</sup> The bacterial flagella can be further assembled into higher ordered structures by forming liquid crystal<sup>47</sup> or by the display of cysteine residues to generate stable nanostructures.<sup>16</sup>

Ribbon-like flagella tight bundles could be rarely observed directly when flagella displaying E8 with a high concentration was incubated in supersaturate HAP solution. They might be formed by super-flagella (spontaneously aggregated thick flagella bundles).<sup>48</sup> SAED pattern also revealed short arcs corresponding to the (002) and (004) planes of HAP, indicating the preferred orientation along the long axis of the flagella bundles (Figure S8).

## CONSLUSIONS

In conclusion, different domains from type I collagen and BSP were successfully displayed on the surface of flagella without losing the motile function. HAP nanocrystals can be nucleated on the surface of engineered flagella displaying either E8 or GPP8 sequences. Oriented nucleation of HAP polycrystalline were observed on the E8 flagella after they are assembled into bundles. The preferred orientation of HAP crystals in the flagella bundles resembles that in the mineralized collagen fibrils in bone which mimic some aspects of the lowest level of ECM. The ease of displaying a functional peptide on the scaffold by genetic means will enable us to introduce functional peptide motifs derived from bone proteins, providing the scaffold with more biological functions needed for bone formation.

## Supplementary Material

Refer to Web version on PubMed Central for supplementary material.

## Acknowledgments

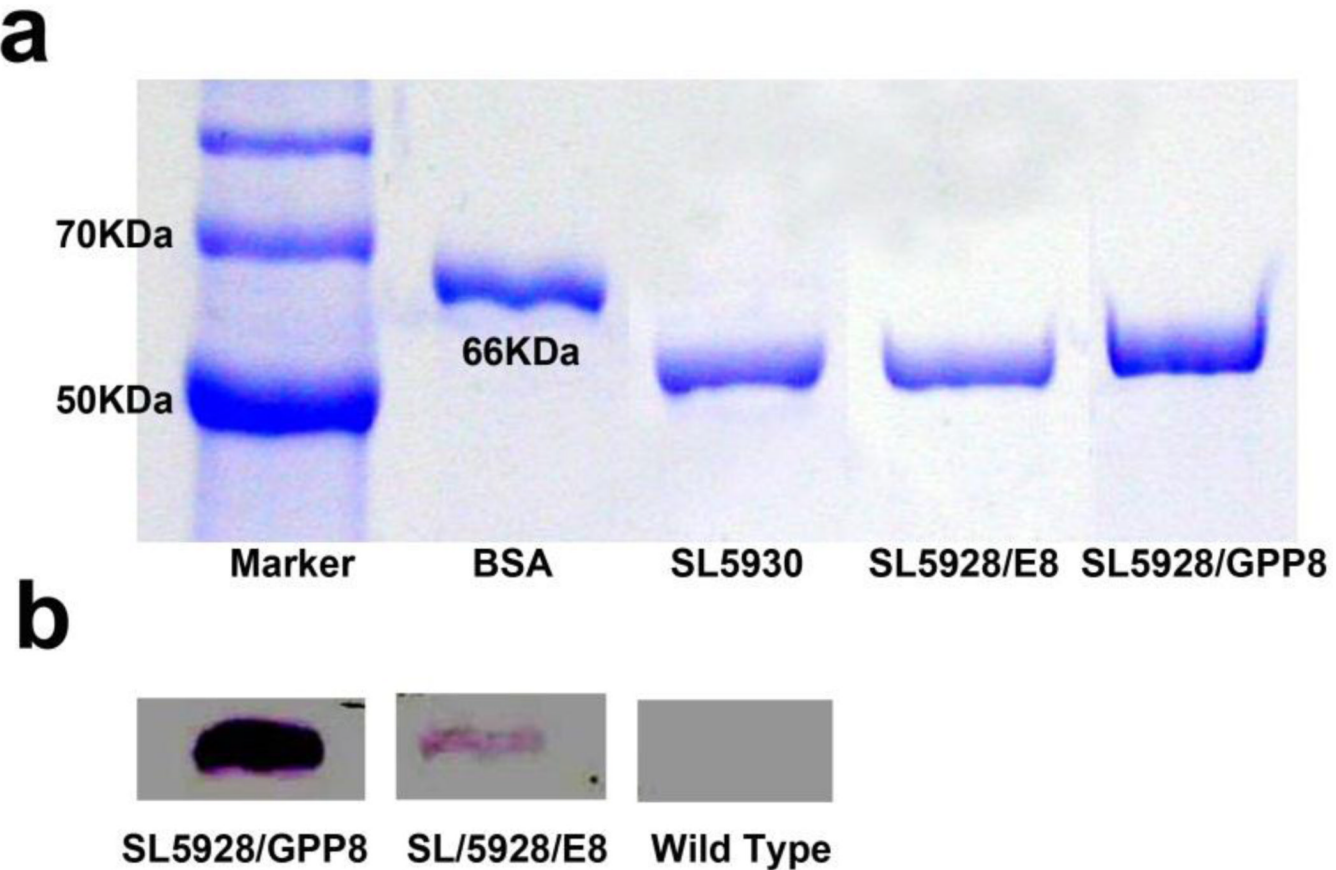
We would like to thank the financial support from National Science Foundation (DMR-0847758, CBET-0854414, CBET-0854465 and CMMI-1234957), National Institutes of Health (5R01HL092526-02, 5R01DE01563309, 5R21EB009909-02, 1R21EB015190-01A1, and 4R03AR056848-03), Oklahoma Center for the Advancement of Science and Technology (HR11-006) and Oklahoma Center for Adult Stem Cell Research (434003).

## REFERENCES

1. George A, Ravindran S. Protein templates in hard tissue engineering. *Nano Today*. 2010; 5:254–266. [PubMed: 20802848]
2. Weiner S, Traub W. Crystal size and organization in bone. *Connect Tissue Res*. 1989; 21:259–265. [PubMed: 2605950]
3. Murphy WL, Mooney DJ. Molecular-scale biomimicry. *Nat Biotechnol*. 2002; 20:30–31. [PubMed: 11753357]
4. Brinckmann, J.; Holger, N.; K, MP. Collagen: primer in structure, processing, and assembly. Vol. Vol. 247. Berlin (DE): Springer; 2005. p. 1-56.
5. Rossert J, de Crombrugghe B. Type I collagen: Structure, synthesis, and regulation. *Principles of Bone Biology*. 1996:127–142.
6. Taton TA. Nanotechnology. Boning up on biology. *Nature*. 2001; 412:491–492. [PubMed: 11484032]
7. Sarikaya M, Tamerler C, Jen AK, Schulten K, Baneyx F. Molecular biomimetics: nanotechnology through biology. *Nat Mater*. 2003; 2:577–585. [PubMed: 12951599]

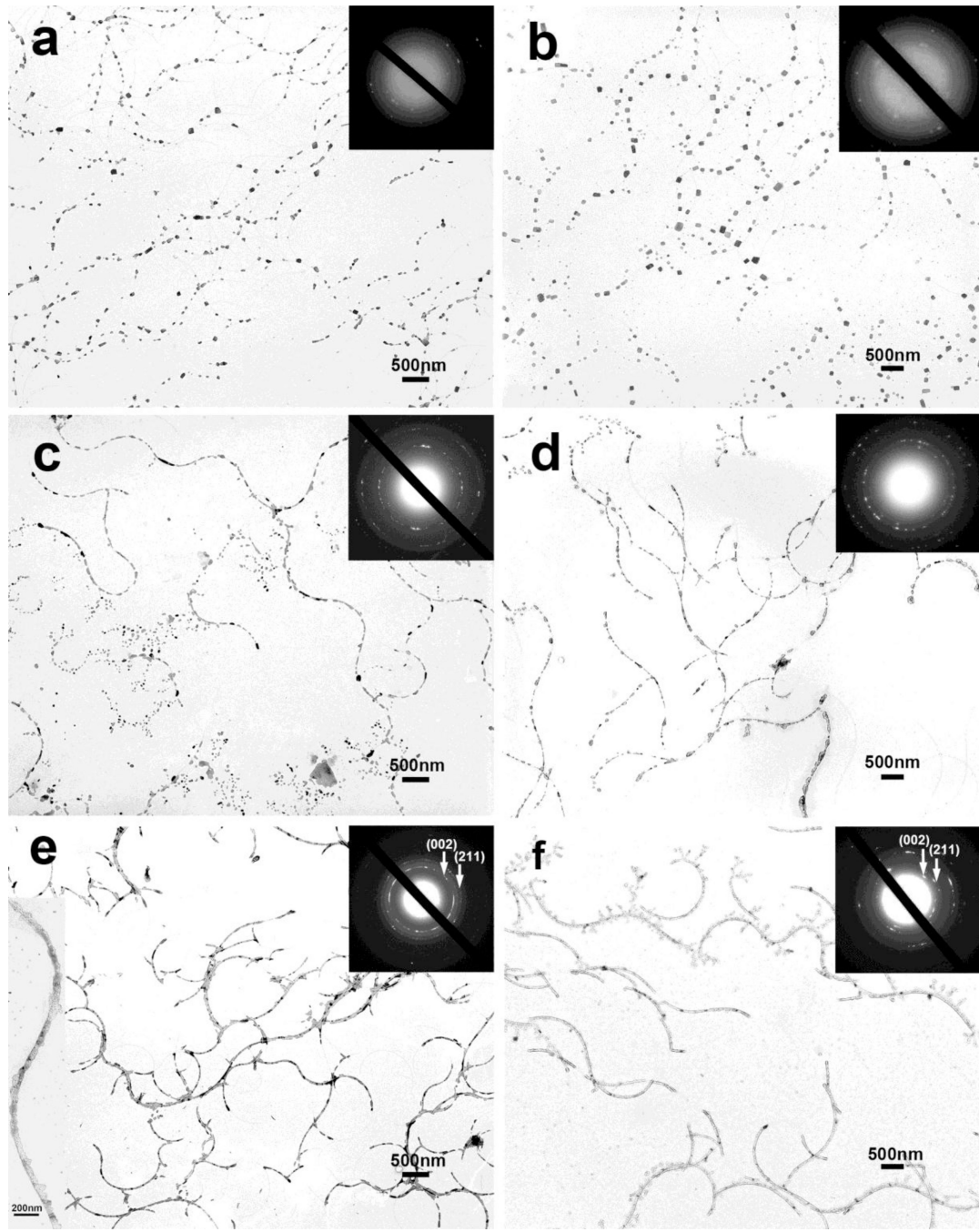
8. He T, Abbineni G, Cao B, Mao C. Nanofibrous Bio-inorganic Hybrid Structures Formed Through Self-Assembly and Oriented Mineralization of Genetically Engineered Phage Nanofibers. *Small*. 2010; 6:2230–2235. [PubMed: 20830718]
9. Cao B, Mao C. Oriented Nucleation of Hydroxylapatite Crystals on Spider Dragline Silks. *Langmuir*. 2007; 23:10701–10705. [PubMed: 17850102]
10. Wang F, Cao B, Mao C. Bacteriophage Bundles with Prealigned Ca<sup>2+</sup> Initiate the Oriented Nucleation and Growth of Hydroxylapatite. *Chem. Mater.* 2010; 22:3630–3636. [PubMed: 20802794]
11. Yonekura K, Maki-Yonekura S, Namba K. Complete atomic model of the bacterial flagellar filament by electron cryomicroscopy. *Nature (London, U.K.)*. 2003; 424:643–650. [PubMed: 12904785]
12. Westerlund-Wikstrom B. Peptide display on bacterial flagella: principles and applications. *Int. J. Med. Microbiol.* 2000; 290:223–230. [PubMed: 10959724]
13. Newton SM, Jacob CO, Stocker BA. Immune response to cholera toxin epitope inserted in *Salmonella* flagellin. *Science*. 1989; 244:70–72. [PubMed: 2468182]
14. Kumara, MTM, Subra; Tripp, Brian C. Generation and Characterization of Inorganic and Organic Nanotubes on Bioengineered Flagella of Mesophilic Bacteria. *Journal of Nanoscience and Nanotechnology*. 2007; 7:2260–2272. [PubMed: 17663239]
15. Kumara MT, Tripp BC, Muralidharan S. Self-Assembly of Metal Nanoparticles and Nanotubes on Bioengineered Flagella Scaffolds. *Chem. Mater.* 2007; 19:2056–2064.
16. Kumara MT, Srividya N, Muralidharan S, Tripp BC. Bioengineered flagella protein nanotubes with cysteine loops: self-assembly and manipulation in an optical trap. *Nano Lett.* 2006; 6:2121–2129. [PubMed: 16968037]
17. Wang F, Li D, Mao C. Genetically Modifiable Flagella as Templates for Silica Fibers: From Hybrid Nanotubes to 1D Periodic Nanohole Arrays. *Adv. Funct. Mater.* 2009; 19:4007–4013.
18. Deplanche K, Woods RD, Mikheenko IP, Sockett RE, Macaskie LE. Manufacture of stable palladium and gold nanoparticles on native and genetically engineered flagella scaffolds. *Biotechnol. Bioeng.* 2008; 101:873–880. [PubMed: 18819156]
19. Hesse WR, Luo L, Zhang G, Mulero R, Cho J, Kim MJ. Mineralization of flagella for nanotube formation. *Materials Science and Engineering: C*. 2009; 29:2282–2286.
20. Zhang W, Liao SS, Cui FZ. Hierarchical Self-Assembly of Nano-Fibrils in Mineralized Collagen. *Chem. Mater.* 2003; 15:3221–3226.
21. Hodge AJ. Molecular models illustrating the possible distributions of 'holes' in simple systematically staggered arrays of type I collagen molecules in native-type fibrils. *Connect Tissue Res.* 1989; 21:137–147. [PubMed: 2605937]
22. Landis WJ, Silver FH, Freeman JW. Collagen as a scaffold for biomimetic mineralization of vertebrate tissues. *J. Mater. Chem.* 2006; 16:1495–1503.
23. Maitland ME, Arsenault AL. A correlation between the distribution of biological apatite and amino acid sequence of type I collagen. *Calcif. Tissue Int.* 1991; 48:341–352. [PubMed: 2054719]
24. Landis WJ, Silver FH. Mineral Deposition in the Extracellular Matrices of Vertebrate Tissues: Identification of Possible Apatite Nucleation Sites on Type I Collagen. *Cells Tissues Organs*. 2009; 189:20–24. [PubMed: 18703872]
25. Salgado AJ, Coutinho OP, Reis RL. Bone tissue engineering: state of the art and future trends. *Macromol. Biosci.* 2004; 4:743–765. [PubMed: 15468269]
26. Wiesmann HP, Meyer U, Plate U, Hoehling HJ. Aspects of collagen mineralization in hard tissue formation. *Int. Rev. Cytol.* 2005; 242:121–156. [PubMed: 15598468]
27. Rhee S-H, Lee JD, Tanaka J. Nucleation of hydroxyapatite crystal through chemical interaction with collagen. *J. Am. Ceram. Soc.* 2000; 83:2890–2892.
28. Hunter GK, Hauschka PV, Poole AR, Rosenberg LC, Goldberg HA. Nucleation and inhibition of hydroxyapatite formation by mineralized tissue proteins. *Biochem. J.* 1996; 317(Pt 1):59–64. [PubMed: 8694787]
29. Hoang QQ, Sicheri F, Howard AJ, Yang DSC. Bone recognition mechanism of porcine osteocalcin from crystal structure. *Nature (London, United Kingdom)*. 2003; 425:977–980. [PubMed: 14586470]

30. Harris NL, Rattray KR, Tye CE, Underhill TM, Somerman MJ, D'Errico JA, Chambers AF, Hunter GK, Goldberg HA. Functional analysis of bone sialoprotein: identification of the hydroxyapatite-nucleating and cell-binding domains by recombinant peptide expression and site-directed mutagenesis. *Bone*. 2000; 27:795–802. [PubMed: 11113390]
31. He G, Dahl T, Veis A, George A. Nucleation of apatite crystals in vitro by selfassembled dentin matrix protein 1. *Nature Materials*. 2003; 2:552–558.
32. Hartgerink JD, Beniash E, Stupp SI. Self-assembly and mineralization of peptideamphiphile nanofibers. *Science*. 2001; 294:1684–1688. [PubMed: 11721046]
33. Hunter GK, Goldberg HA. Modulation of crystal formation by bone phosphoproteins: role of glutamic acid-rich sequences in the nucleation of hydroxyapatite by bone sialoprotein. *Biochem. J.* 1994; 302(Pt 1):175–179. [PubMed: 7915111]
34. Tye CE, Rattray KR, Warner KJ, Gordon JA, Sodek J, Hunter GK, Goldberg HA. Delineation of the hydroxyapatite-nucleating domains of bone sialoprotein. *J. Biol. Chem.* 2003; 278:7949–7955. [PubMed: 12493752]
35. Goldberg HA, Warner KJ, Stillman MJ, Hunter GK. Determination of the hydroxyapatite-nucleating region of bone sialoprotein. *Connect Tissue Res.* 1996; 35:385–392. [PubMed: 9084679]
36. De Almeida MES, Newton SM, Ferreira LCS. Antibody responses against flagellin in mice orally immunized with attenuated *Salmonella* vaccine strains. *Arch. Microbiol.* 1999; 172:102–108. [PubMed: 10415171]
37. Wang Y, Yang C, Chen X, Zhao N. Biomimetic formation of hydroxyapatite/collagen matrix composite. *Adv. Eng. Mater.* 2006; 8:97–100.
38. Gajardo R, Vende P, Poncet D, Cohen J. Two proline residues are essential in the calcium-binding activity of rotavirus VP7 outer capsid protein. *J. Virol.* 1997; 71:2211–2216. [PubMed: 9032355]
39. Mattice WL, Mandelkern L. The Conformational Transition Induced in Poly(4-hydroxy-L-proline) by Calcium Chloride. *Macromolecules*. 1970; 3:199–201.
40. Chung W-J, Kwon K-Y, Song J, Lee S-W. Evolutionary Screening of Collagenlike Peptides That Nucleate Hydroxyapatite Crystals. *Langmuir*. 2011;7620–7628. [PubMed: 21291244]
41. Zhang W, Huang Z-L, Liao S-S, Cui F-Z. Nucleation Sites of Calcium Phosphate Crystals during Collagen Mineralization. *J. Am. Ceram. Soc.* 2003; 86:1052–1054.
42. Tye CE, Hunter GK, Goldberg HA. Identification of the Type I Collagen-binding Domain of Bone Sialoprotein and Characterization of the Mechanism of Interaction. *J. Biol. Chem.* 2005; 280:13487–13492. [PubMed: 15703183]
43. Toworfe GK, Composto RJ, Shapiro IM, Ducheyne P. Nucleation and growth of calcium phosphate on amine-, carboxyl- and hydroxyl-silane self-assembled monolayers. *Biomaterials*. 2006; 27:631–642. [PubMed: 16081155]
44. Goldberg HA, Warner KJ, Li MC, Hunter GK. Binding of bone sialoprotein, osteopontin and synthetic polypeptides to hydroxyapatite. *Connect Tissue Res.* 2001; 42:25–37. [PubMed: 11696986]
45. Strzelecka-Golaszewska H, PrÓChniewicz E, Drabikowski W. Interaction of Actin with Divalent Cations. *Eur. J. Biochem.* 1978; 88:219–227. [PubMed: 566667]
46. Wakabayashi K, Hotani H, Asakura S. Polymerization of salmonella flagellin in the presence of high concentrations of salts. *Biochimica et Biophysica Acta (BBA) - Protein Structure*. 1969; 175:195–203.
47. Barry E, Hensel Z, Dogic Z, Shribak M, Oldenbourg R. Entropy-driven formation of a chiral liquid-crystalline phase of helical filaments. *Phys Rev Lett.* 2006; 96:018305. [PubMed: 16486530]
48. Alam M, Oesterhelt D. Morphology, function and isolation of halobacterial flagella. *J. Mol. Biol.* 1984; 176:459–475. [PubMed: 6748081]
49. Lu HB, Ma CL, Zhou HCLF, Wang RZ, Cui FZ. Controlled crystallization of calcium phosphate under stearic acid monolayers. *J. Cryst. Growth*. 1995; 155:120–125.
50. Kamiya R, Asakura S. Flagellar transformations at alkaline pH. *J. Mol. Biol.* 1976; 108:513–518. [PubMed: 13224]

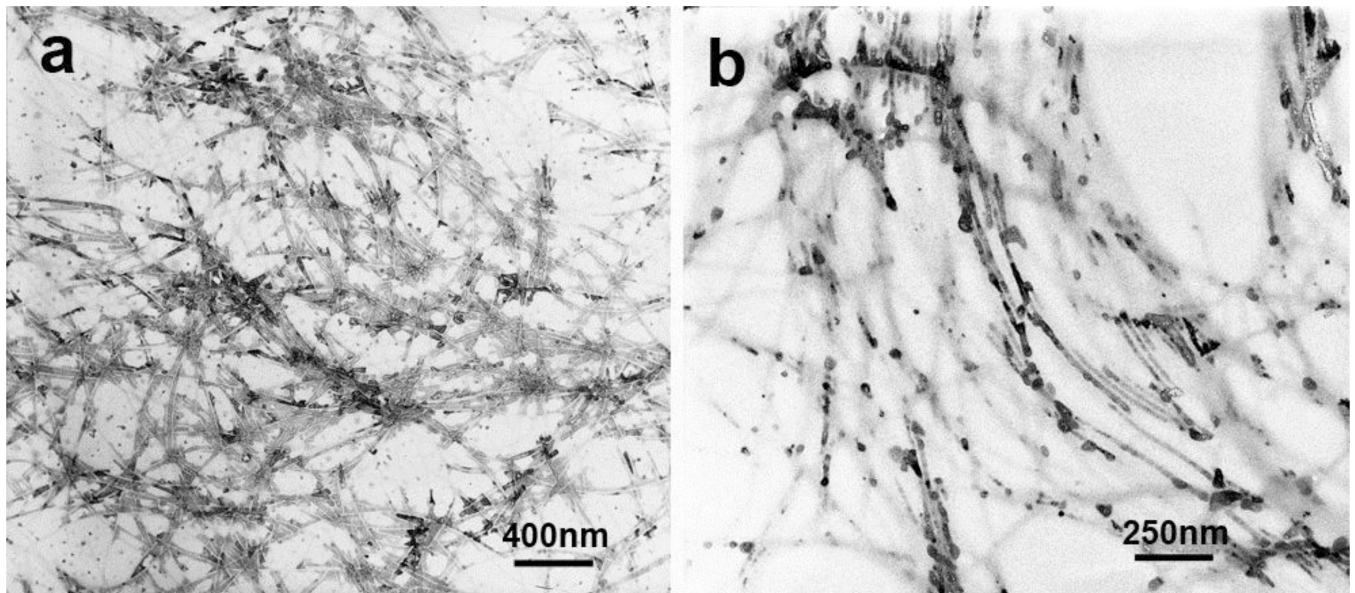


**Figure 1.**

(a) SDS-PAGE electrophoresis of flagellin (8  $\mu$ L/sample). Molecular weight of BSA is 66 kDa. SL5930 encodes flagellin protein with a 48bp deletion in the center of hypervariable region (Control). The molecular weights of SL5928/E8 and SL5928/GPP8 are close to that of SL5930. (b) Western blotting of recombinant flagellin. A clear band can be observed for SL5928/GPP8 and SL5928/E8. Wild type flagellin was used as a control.

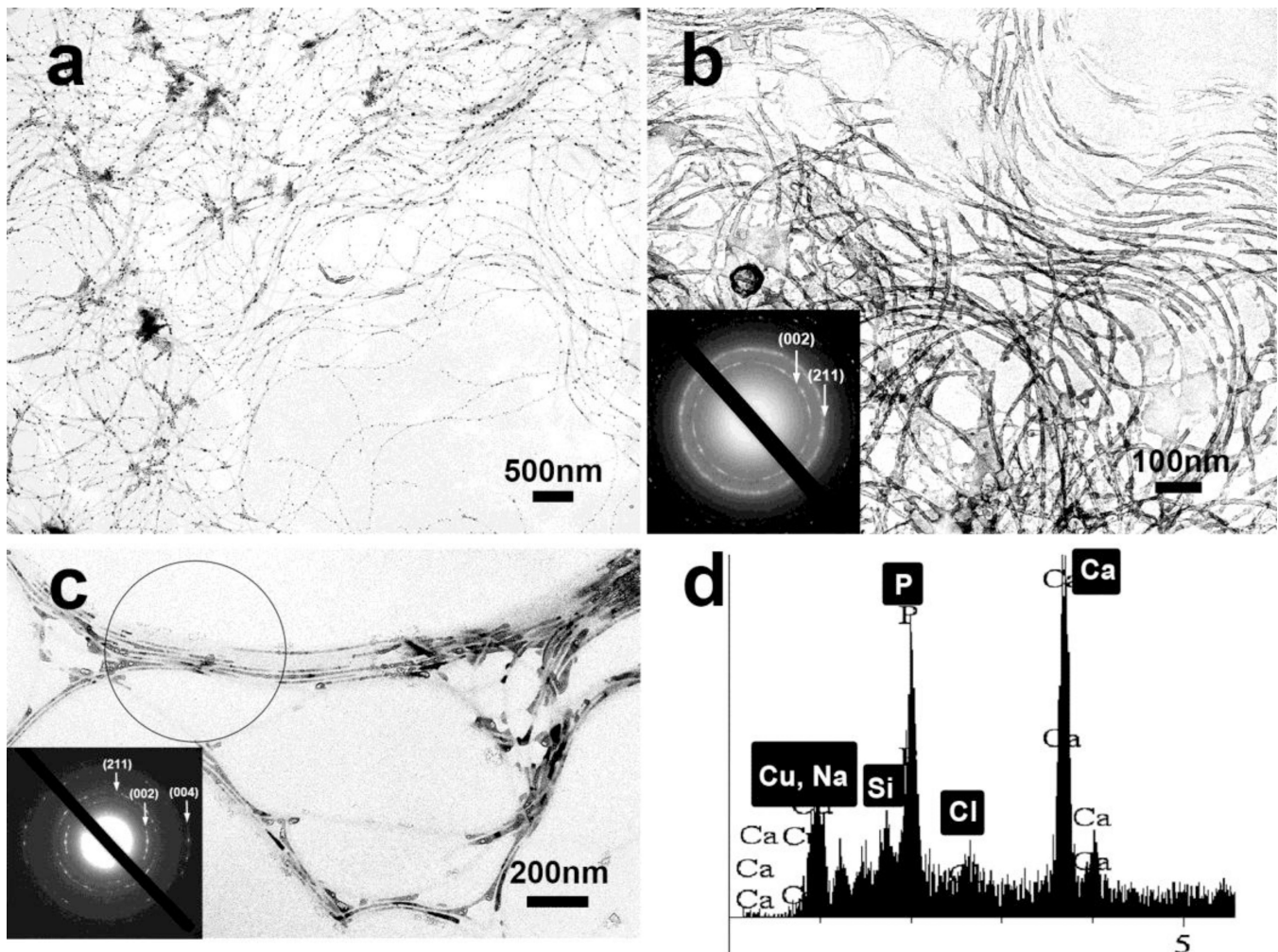


**Figure 2.**  
TEM images and SAED patterns of flagella displaying E8 or GPP8 (2  $\mu\text{g}/\text{mL}$ ) after mineralized in 4 mM supersaturated HAP precursor solution at different time intervals. (a, b) After 3 days, flagella displaying E8 (a) and GPP8 (b) in supersaturated HAP solution. Less crystalline minerals were nucleated. (c, d) After 6 days, flagella displaying E8 (c) and GPP8 (d). Some crystalline HAP minerals were nucleated. (e, f) After 9 days, flagella displaying E8 (e) with high magnification (inset) and GPP8 (f). More HAP crystals were nucleated on the surface of flagella. Flagella displaying E8 had much stronger SAED pattern than those displaying GPP8.

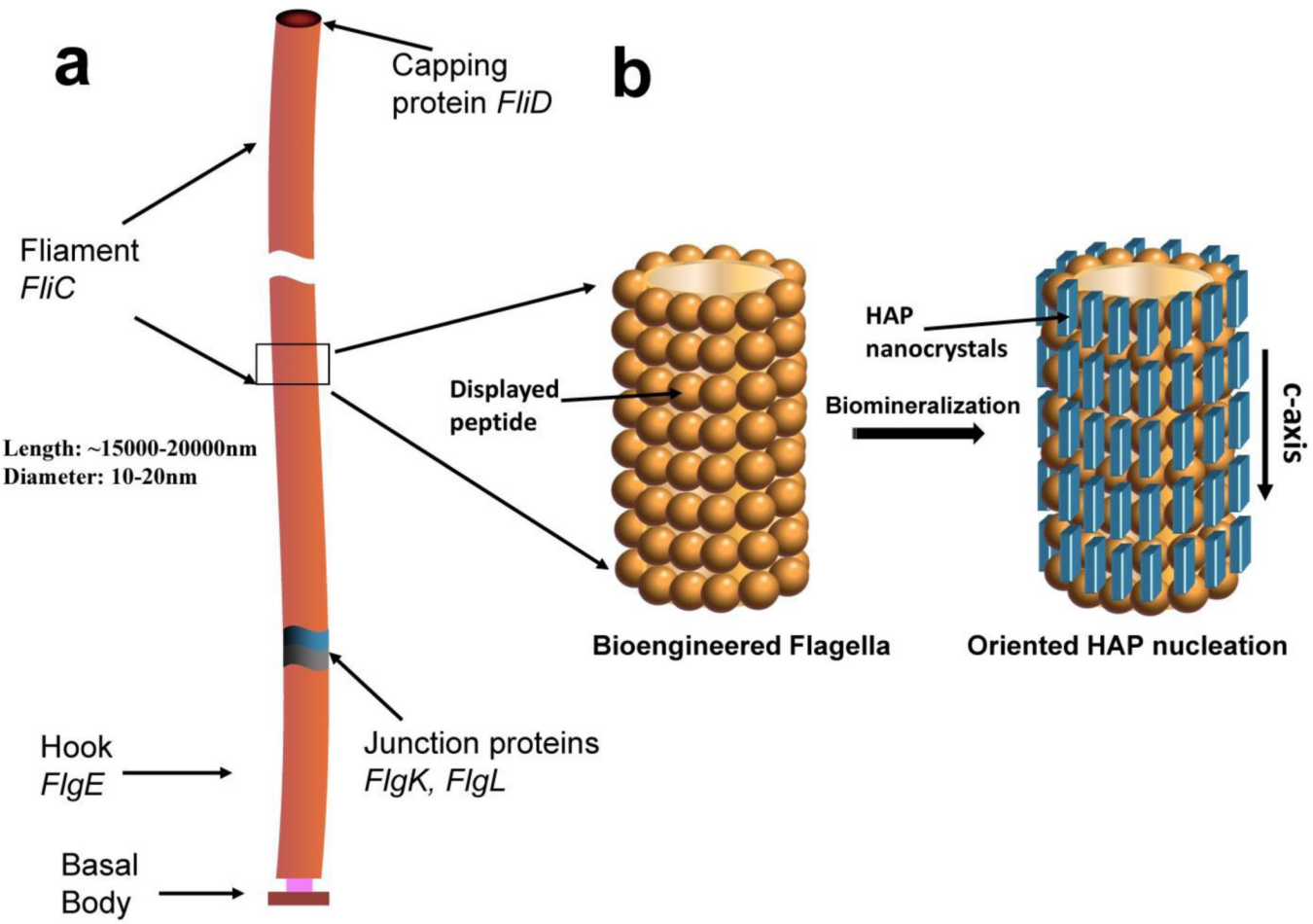


**Figure 3.**

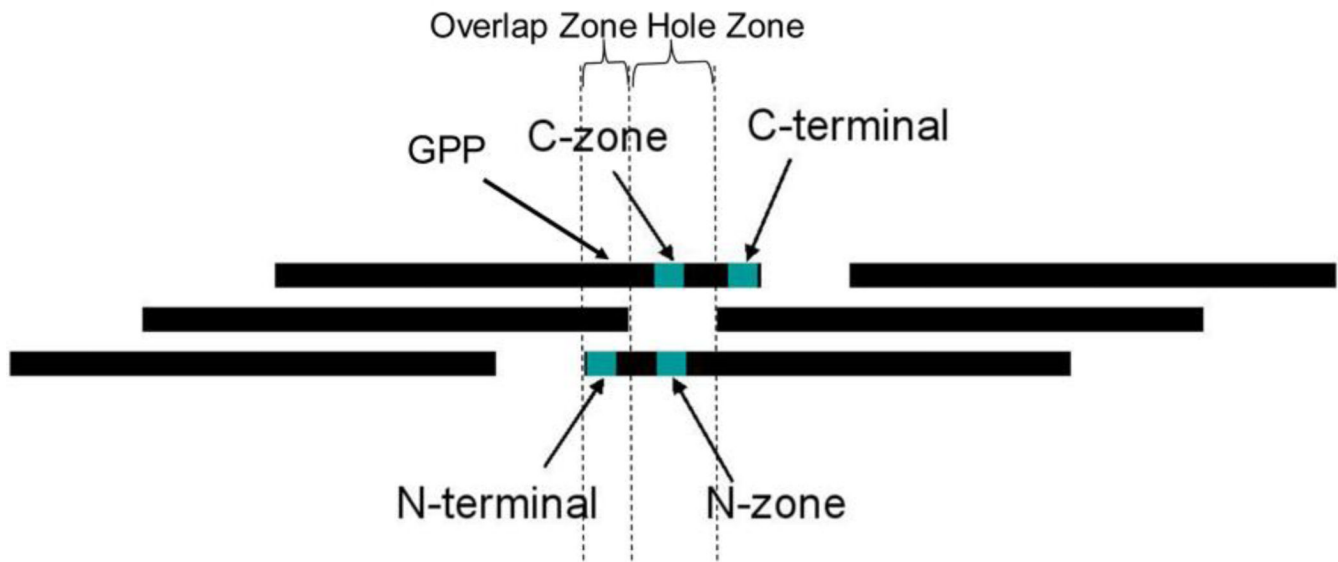
TEM images of flagella with higher concentration ( $10 \mu\text{g/mL}$ ) with E8 displayed after mineralized in 4 mM supersaturated HAP precursor solution for 9 days. (a) Bundle-like structures of flagella can be observed at some areas. (b) High magnification of bundle-like flagella.



**Figure 4.**  
TEM images of flagella bundles displaying E8 induced by calcium ions followed by mineralization in supersaturated HAP solution with EDS and SAED analysis. (a) 1 day after flagella bundles were mineralized in supersaturated HAP solution. Nanoscale minerals were nucleated on the surface of flagella. (b) 3 days after flagella bundles were mineralized in supersaturated HAP solution. The bundles became “loose” and were decorated by a layer of HAP nanocrystals. (c) Narrow flagella bundles with SAED pattern (insert) taken from the highlighted section. The arcs (002) and (004) indicated the c-axis oriented nucleation of HAP. (d) EDS analysis of the flagella bundles.

**Scheme 1.**

(a) Illustration of flagella structure and (b) Oriented nucleation of HAP on the surface of bioengineered flagella.



**Scheme 2.**

Positions of different regions within type I collagen in bone. N, C-zones located at the hole zone were selected. N, C- terminals located at the overlap zone were selected. Some GPP repeats are located at the overlap zone. Some of them are located at the hole zone.

Table 1

Inserted sequences in recombinant plasmid and peptides displayed on flagella as well as the resultant nucleation behavior on the flagellar surface.